AEDC-TR-70-246

cy. 3

EXPERIMENTAL EVALUATION OF A THRUST VECTOR LOAD CELL

R. W. Postma

Rockketdyne

November 1970

ARNOLD ENGINEERING DEVELOPMENT CENTER
AIR FORCE SYSTEMS COMMAND
ARNOLD AIR FORCE STATION, TENNESSEE

NOTICES

EXPERIMENTAL EVALUATION OF A THRUST VECTOR LOAD CELL

R. W. Postma
Rockétdyne

FOREWORD

The work presented herein was sponsored by Arnold Engineering Development Center (AEDC), Air Force Systems Command (AFSC), Arnold Air Force Station, Tennessee, under Program Element 65701F, Project 4344, Task 37.

This report was prepared by the Research Division of Rocketdyne, a Division of North American Rockwell Corporation, Canoga Park, California, under Air Force Contract F40600-70-C-0007, "Research Contract for the Evaluation of a Thrust Vector Load Cell." The contract consisted of the instrumentation and calibration of a half-scale model previously fabricated and partially strain gaged under Contract F40600-68-C-0004, "Research of a Vector Thrust Load Cell," Report No. AEDC-TR-64-233. Inclusive dates of the present evaluation were November 1969 to February 1970. This report has been designated R-8254 by Rocketdyne. The manuscript was submitted for publication 15 June 1970.

The author is particularly indebted to J. LeFevere and others associated with the NAR Tri-Sonic Wind Tunnel Facility who provided invaluable advice and assistance in the calibration of the model.

The reproducibles used in the reproduction of this report were supplied by the authors.

This technical report has been reviewed and is approved.

David G. Francis
First Lieutenant, USAF
Research and Development Division
Directorate of Technology

Harry L. Maynard
Colonel, USAF
Director of Technology

ABSTRACT

This report describes the results of an experimental evaluation of a half-scale (physical size) model of a previously analyzed six-component force balance for testing rocket engines. The force range of the model was scaled down from 5000 lb_f to 200 lb_f, and structural parameters were scaled to represent those of the full-scale version which was analyzed under Contract F40600-68-C-0004. The evaluation includes the determination of (1) first- and second-order interactions of single and combination loads and (2) the effect of combination loads at expected gimbal points for typical rocket engines. The data which are presented in tabulated form, validate the prior analysis, and demonstrate that short force measuring links, assembled into a compact integral structure, do not result in excessive interactions.

CONTENTS

ILLUSTRATIONS

TABLES

SECTION I

SUMMARY

This evaluation of a scale model vector thrust load cell has served to validate the analytical study of the concept of using an integral force balance for measuring rocket engine thrust. The precision of the model demonstrated capability to exceed the $1/3^{\circ}$ vector angle final accuracy goal by an order of magnitude and readily achieve the 0.020-inch vector location and 1/2 percent thrust amplitude accuracy goals of the preceding contract.

The basic structure of the design tested showed that it is feasible to build a balance comprised of short, rigid force-measuring links assembled into a compact structure located at the front of the rocket motor. The balance tested in this program was purposely designed to demonstrate the capability to achieve low interactions between the axial force links and the side force links. The design was intentionally kept elementary so as to make its understanding and analysis as simple as possible.

Having demonstrated these objectives, it is worthwhile to reflect on the importance of low interactions. Although such qualities as low interaction and linearity are the usual criteria for a successful six-component force balance, accurate results can be achieved if relatively large first-order interactions and non-linearities are repeatable, can be accurately evaluated by proper calibration, and can be corrected for in the reduction of test data. From a practical point of view, second-order interactions caused by balance distortion under load should be small because many combinations of calibration

loads are needed to evaluate them. The second-order interactions in this testing were demonstrated to be insignificant as predicted by the previous analysis.

In contrast to other balance geometries analyzed in the previous study (Ref. 1), it is a characteristic of the balance design tested that the precision of vector location depends primarily on force link precision rather than on the structural geometry. The precision achieved during this testing did not reach the ultimate precision capabilities of high precision load cells or wind tunnel balances although the vector location and magnitude precision were well within the objectives of this program. As discussed in the preceding study, important factors in this concept are (1) the convenience of being able to evaluate interactions on the special calibration rig prior to aligning the balance to the engine, (2) the ability to assemble the balance and engine on the test stand, and (3) the ability to perform final calibrations before and after test firing. As discussed in the section on results, the improvement of force cell precision is partly a matter of reducing strain-gage creep and further refinement of calibration technique.

SECTION II

INTRODUCTION

In rocket engine development and production acceptance static testing it is frequently essential that the magnitude, direction, and location of the net thrust vector be determined. This is currently accomplished through use of multi-component thrust stands comprised of externally arranged load-measuring assemblies. Because of the obvious operational shortcomings of such arrangements, the idea of a single transducer which could be used to obtain thrust vector data has long been attractive. But there was little progress toward achieving such a device until the Arnold Engineering Development Center sponsored the analytical evaluation of the concept in 1968 under Contract F40600-68-C-0004.

The conclusions from this study (Ref. 1) indicated that a vector thrust load cell with an integral propellant compensator is capable of providing the general advantages of:

1. Reduced on-site calibration effort
2. Simplified alignment of the rocket engines
3. Improved thrust measurement accuracy for liquid propellant rockets.

Because of the unorthodox force link geometries, the short force link lengths, and the stiff flexures and force links that were incorporated in the basic concept analyzed; an experimental evaluation of a model transducer was recommended. This report describes the experimental program which was carried out to confirm the analytical conclusions.

SECTION III

DESCRIPTION OF APPARATUS

3.1 MODEL CELL

A thrust cell for use over a range of 1000 to 20,000 pounds of axial force at vector angles up to 12° was considered for the analytical study. A model cell (Fig. 1) based on the following design and scaling considerations, was completed and used for the experimental evaluation.

1. The dimensions which establish kinematic relationships are half of those specified for the full-scale basic design. These dimensions are lengths of force links, positions of force links, and plate diameter. The overall size of the model is 7-1/8 inches diameter by 3-3/4 inches.

2. Load capacity was scaled down 25:1. Nominal axial thrust capacity of the model is 200 lb_f compared to 5000 lb_f and side thrust capacity of 40 lb_f compared to 1000 lb_f.

3. The reduced load capacity allowed use of flexures machined as two short small diameter rods near the end of each force link. Because each of these rod flexures provides three degrees of freedom, the total number of flexures is reduced in the ratio of 5:2 compared to the full-scale design (where four circular flexures and one cruciform torsion flexure are needed per force link).

4. Restoring moments caused by bending and torsion of the rod flexures are approximately the same percentage of applied forces as the circular arc flexures used in the full-scale design. Because rod flexures are much stiffer in bending than circular arc flexures, the reduced loads were necessary to allow the cross-sectional areas of the rods to be scaled down. The result is that the relative bending stiffness (also referred to as percentage redundancy) of the half-scale model is the same as the full-scale design.

5. Non-linear, second-order interactions are also designed to be the same as in the full-scale version. Consequently, angular distortion of the balance under nominal load is the same. To accomplish this, compression and tension deflections of flexures and force cells, machined as part of each force link, are scaled to one-half at nominal load (approximately 0.001 inch vs. 0.002 inch). The thickness of the two circular plates and the size of brackets supporting side force links were also scaled so that calculated plate and bracket deflections are reduced to one-half at nominal loads.

6. Force cells, as well as flexures, were machined as integral parts of the force links. The force cells are short columns with "I" cross sections that are strained in compression or tension. Strain gages can be bonded to either the webs or the outsides of the flanges of the axial force cells (L_1, L_2, and L_3). The side force cells have sufficient space for strain gages on the flanges only.

7. The force links, plates, and brackets were machined from 17-4 PH corrosion-resistant steel, the same material which would be used for a full-scale working model. Force links were age-hardened after partial machining to achieve the high yield strength needed for repeatable stress-strain characteristics in force cells and flexures.

8. Semi-conductor strain gages were bonded to the three axial force links, L_1, L_2, and L_3 (Fig. 2) and the side force link, L_4. These strain gages were wired into Wheatstone bridge circuits and temperature compensated as usual.

9. The alignment of the axial load and side load to the reference plane was controlled by the use of precision levels. The precision of the level used to align the space of the cell has a resolution of .00002 radians. The level used to align the axial force rod has a resolution of .00008 radians. During the application of loads to the balance, the base of the balance was realigned by observing these two levels to compensate for balance and support deflections.

3.2 CALIBRATION RIG

The calibration rig used for this work is the wind tunnel balance certification equipment at the North American Rockwell Corporation, Los Angeles Division, Tri-Sonic Wind Tunnel. In addition to the high precision alignment fixtures, this system has digital readout instruments for use with strain gages.

The model cell is shown mounted on the movable sling of the calibration rig in Fig. 3.

SECTION IV

CALIBRATION AND DATA REDUCTION PROCEDURES

Calibration constants including correction terms for first-order interactions were obtained by applying loads directly in line with the four strain-gaged force links (L_1, L_2, L_3, and L_4 of Fig. 1).

The data reduction was accomplished using existing computer programs at the Tri-Sonic Wind Tunnel. Least squares second-degree best-fit curves were obtained for the primary constants and first-degree curves for the interaction terms. For loadings at other points than the four force links, pseudo[1]-reaction forces at the four calibration load stations were obtained from the following equations.

$$
\begin{aligned}
R_1 &= (B_{11}E_1 + C_{11}E_1^{2}) + M_{12}R_2 + M_{13}R_3 + M_{14}R_4 \\
R_2 &= M_{21}R_1 + (B_{22}E_2 + C_{22}E_2^{2}) + M_{23}R_3 + M_{24}R_4 \\
R_3 &= M_{31}R_1 + M_{32}R_2 + (B_{33}E_3 + C_{33}R_3^{2}) + M_{34}R_4 \\
R_4 &= M_{41}R_1 + M_{42}R_2 + M_{43}R_3 + (B_{44}E_4 + C_{44}E_4^{2})
\end{aligned}
\tag{1}
$$

In these equations the R_i terms are forces at the four load stations in line with the force links, and the E_i terms are the electrical outputs in millivolts. The B_{ii} and C_{ii} terms are constants describing the calibration curves obtained from calibration loads over the respective force link L_i (lb-volts/mv and lb-volts^2/mv^2 respectively). The M_{ij} terms are considered

[1] The reaction forces may be considered to exist at these points although the input forces are reacted at the actual force link locations.

to be interaction terms with reference to these four load stations (lb/lb).

These terms represent the partial derivatives of applied calibration force to the apparent force indicated at another load station and are computed from the calibration data by:

$$M_{ij} = \frac{B_{ii}}{B_{ij}} \tag{2}$$

Here the B_{ij} terms are the interaction slopes from the calibrations in lb-volts/mv.

Since the objective of the data reduction is to compute the magnitude, direction, and location of the external force vector, another set of equations is written to translate the pseudo-reaction forces obtained by solution of the preceding equations for cases where an axial load at the center is combined with a side load at some known distance from the center of the balance. The first set of equations was solved by iteration, using the standard computer program and the resulting reaction forces were entered into the following set of equations:

$$F_z = R_1 + R_2 + R_3 \qquad X_1 = .009 \text{ inch} \tag{3}$$

$$F_x = R_4 \qquad X_2 = 2.167 \text{ inch}$$

$$M_y = R_1 x_1 + R_2 x_2 + R_3 x_3 \qquad X_3 = -2.161 \text{ inch}$$

$$F = \sqrt{F_x^2 \quad F_z^2}$$

$$\theta = \text{arc tan } \frac{F_x}{F_z}$$

$$\bar{x} = \frac{M_y}{F_z}$$

By this method the strain gage voltages E_i produced by known input forces F_z and F_x have been used to compute reaction forces R_i at the calibration load stations which are then translated to the calculated external thrust vector for comparison with the known thrust vector.

SECTION V

RESULTS

5.1 CALIBRATION CONSTANTS

The calibration constants obtained in this experiment are given in Table I in matrix form.

TABLE I

CALIBRATION CONSTANTS

B_{11} = -11.8408 C_{11} = .01191	M_{12} = .00723	M_{13} = -.00243	M_{14} = .000017
M_{21} = -.000657	B_{22} = -13.2367 C_{22} = .01642	M_{23} = -.00489	M_{24} = .001386
M_{31} = .00301	M_{32} = .00731	B_{33} = -12.1871 C_{33} = .01444	M_{34} = .001496
M_{41} = .000269	M_{42} = .000418	M_{43} = .000260	B_{44} = 11.5535 C_{44} = .00375

5.2 TABULATED RESULTS

Table II compares the measured values of thrust vector magnitude angle and location (corrected for first-order interactions from Table I) with the calibration inputs of the same parameters.

SECTION VI

DISCUSSION OF RESULTS

6.1 ANGULAR PRECISION

The experimental results satisfactorily accomplished the main objective of this program: that of evaluating the basic design described as the orthogonal tripod geometry in Ref. 1. Most noteworthy, the first-order interactions resulting from force link misalignment were very small and were readily corrected for as a routine procedure in data reduction. Also, the second-order interactions caused by angular distortion of force links under load were sufficiently small that very high angular precision was achieved by accounting for only the first-order interactions. The angular measurements would still have been very precise if the first-order interactions were also ignored.

The interaction caused by misalignment of the axial force links (see Section 7.2.1, Ref. 1) is given by the sum of $M_{41} + M_{42} + M_{43}$ in the calibration matrix (Table I) which is equal to .0003 radians for a purely axial load. The results corrected for this interaction (shown in Table II) gave a 2 σ[2] error of .00016 radian for all purely axial loads ($\theta = 0$) and .00036 radian for all load combinations including angles up to 22° of arc. The maximum error as shown in the tabulated results in Table II was .00047 radian at 11.5°.

During the combination load tests the side loads were applied at a station representing a typical gimbal location. This location of $\bar{z} = 6.255$ inches from the center of the balance would be equivalent to 12.510 inches in a full-scale model.

[2]Twice the standard deviation represents a probability of .95 that an individual error will be less than the 2σ error (for large sample uses). This is sometimes stated as the 95% confidence level.

TABLE II

RESULTS
(Corrected For First Order Interactions)

Run No.	INPUT PARAMETERS: AXIAL FORCE F_a lb_f	SIDE FORCE F_x lb_f	ANGLE ϕ Degrees	LOCATION $\bar{s}$ Inches	LOCATION $\bar{x}$ Inches	RESULTANT FORCE F lb_f	MEASURED ANGLE: ANGLE θ Radians	ERROR θ Degrees	ERROR θ Radians	MEASURED FORCE: RESULTANT FORCE F lb_f	ERROR F % OF READING	MEASURED LOCATION (IN xy PLANE): LOCATION $\bar{x}$ Inches	ERROR AS MEASURED $\bar{x}$ Inches	ERROR ADJUSTED FOR: FLEXURE* DISTORTION $\bar{x}$ Inches	BIAS $\bar{x}$ Inches
12	50	0	0	N.A.	0	50	.00002	-	.00002	50.038	.076	-.0102	-.0102	-.0022	.0002
	100	0	0	N.A.	0	100	.00008	-	.00008	99.998	-.002	-.0107	-.0107	-.0027	-.0003
	200	0	0	N.A.	0	200	.00005	-	.00005	199.819	-.090	-.0106	-.0106	-.0026	-.0002
	300	0	0	N.A.	0	300	.00001	-	.00001	300.004	.001	-.0105	-.0105	-.0025	-.0001
	400	0	0	N.A.	0	400	-.00002	-	-.00002	400.142	.036	-.0101	-.0101	-.0021	.0003
												Average =	-.0104,	-.0024	
	The remaining data were taken on the following day. Calibrations over force lines L_1, L_2, and L_3 were performed in Runs 13, 14, and 15 of the preceding day.														
17	50	0	0	N.A.	0	50	.00008	-	-.00008	50.002	.004	-.0107	-.0107	-.0027	-.0003
	50	5	5.72	6.255	.6255	50.249	.09947	5.70	-.00019	50.188	-.121	.6162	-.0093	-.0013	.0011
	50	10	11.32	6.255	1.2510	50.990	.19691	11.28	-.00047	50.949	-.082	1.2414	-.0095	-.0015	.0009
18	100	0	0	N.A.	0	100	-.00008	-	-.00008	99.928	-.072	-.0102	-.0102	-.0022	.0002
	100	5	2.87	6.255	.3127	100.125	.04970	2.85	-.00025	100.062	-.063	.3022	-.0105	-.0025	-.0001
	100	10	5.72	6.255	.6255	100.499	.09932	5.69	-.00034	100.436	-.062	.6162	-.0093	-.0013	.0011
	100	15	8.53	6.255	.9382	101.119	.14852	8.51	-.00036	101.010	-.107	.9295	-.0087	-.0007	.0017
	100	20	11.32	6.255	1.2510	101.980	.19693	11.28	-.00046	101.840	-.137	1.2433	-.0077	.0003	.0027
	*A bent flexure on the axial force calibration rod was replaced after Run 18.														
19	150	0	0	N.A.	0	150.000	.00018	.01	.00018	150.061	.040	-.0017	-.0017		.0007
	150	10	3.82	6.255	.4169	150.333	.06668	3.82	.00011	150.179	-.102	.4171	.0002		.0026
	150	20	7.60	6.255	.8399	151.327	.13245	7.59	-.00010	151.214	-.075	.8404	.0005		.0029
	150	30	11.32	6.255	1.2510	152.971	.19708	11.29	-.00030	152.800	-.112	1.2517	.0007		.0031
20	200	0	0	N.A.	0	200.000	.00008	-	.00008	199.918	-.041	-.0034	-.0034		-.0010
	200	10	2.87	6.255	.3127	200.249	.04985	2.86	-.00009	200.496	.123	.3127	-.0060		.0024
	200	20	5.72	6.255	.6255	200.996	.09956	5.70	-.00010	200.928	-.034	.6233	-.0022		.0002
	200	30	8.53	6.255	.9382	202.237	.14872	8.52	-.00016	202.066	-.084	.9371	-.0011		.0013
	200	40	11.32	6.255	1.2510	203.961	.19722	11.30	-.00016	203.643	-.155	1.2508	-.0002		.0022
20.1	300	0	0	N.A.	0	300.000	-.00002	-	-.00002	300.128	.043	-.0063	-.0063		-.0039
	300	10	1.91	6.255	.2085	300.167	.03341	1.91	.00009	300.186	.007	.2030	-.0054		-.0030
	300	20	3.82	6.255	.4170	300.666	.06671	3.82	-.00015	300.662	-.001	.4122	-.0048		-.0024
	300	0	0	N.A.	0	300.000	.00003	-	.00003	300.145	.048	-.0060	-.0060		-.0036
20.2	400	0	0	N.A.	0	400.000	.00002	-	.00002	400.194	.049	-.0073	-.0073		-.0049
21	50	0	0	N.A.	0	50	.00008	-	.00006	49.980	-.040	-.0031	.0031		.0055
	100	0	0	N.A.	0	100	.00000	-	.00000	100.030	.030	.0011	.0011		.0035
	150	0	0	N.A.	0	150	-.00002	-	.00002	149.960	-.026	-.0016	-.0016		.0008
	200	0	0	N.A.	0	200	.00014	-	.00014	200.080	.040	-.0038	-.0038		-.0014
23	100	0	0	0	0	100	.00008	-	1.00014	100.155	.155	.0017	.0017		.0041
	100	10	5.72	0	0	100.500	**	**	**	**	**	.0013	.0013		.0037
	100	20	11.32	0	0	101.980	.19736	11.31	-.00002	101.993	.013	.0001	.0001		.0025
	100	30	16.70	0	0	104.403	.29137	16.69	-.00008	104.374	-.026	.0006	.0006		.0030
	100	40	21.80	0	0	107.703	.38050	21.80	.00000	107.583	-.112	.0006	.0006		.0030
24	200	0	0	0	0	200.000	.00005	-	.00005	200.128	.064	-.0032	-.0032		-.0008
	200	10	2.87	0	0	200.250	.05017	2.87	-.00021	200.333	.041	-.0028	-.0028		-.0004
	200	20	5.72	0	0	200.998	.09980	5.72	.00013	201.043	.022	-.0032	-.0032		-.0008
	200	30	8.53	0	0	202.237	.14904	8.54	.00015	202.243	.003	-.0032	-.0032		-.0008
	200	40	11.32	0	0	203.961	.19758	11.32	.00018	203.936	-.012	-.0030	-.0030		-.0006
25	100	20	11.32	3.130	.6260	101.980	.19730	11.30	-.00008	102.018	.037	.6279	.0019		.0043
	100	40	21.80	3.130	1.2520	107.703	.38026	21.79	-.00023	107.642	-.056	1.2542	.0022		.0046
26 ∦	100	20	11.32	9.382	1.876	101.980	.19688	11.28	-.00050	102.020	.039	1.8784	.0020		.0044
	100	40	21.80	9.382	3.752	107.703	.37952	21.74	-.00098	107.571 ≠	-.122 ≠	3.7610 ≠	.0090 ≠		.0114

**Error in data reduction.

≠ Force link L_2 was loaded in tension on this loading, which was beyond the range of the calibration constants used in this data reduction.

∦ These loads at $\bar{s}$ = 9.382 are beyond the normal range of the balance.

15/16

One of the primary questions to be answered in this evaluation was whether or not the side load could be accurately measured when applied at the distance $\bar{z}$ from the side force link. The results verify the analysis in Ref. 1 and show conclusively that the effect of this overhung loading structure is very minimal. In Runs 18, 19, and 20 (Table II) the additional error due to the increase in vector angle from 0 to 11.5° is small enough that the second-order interactions caused by balance distortion (see Section 7.3, Reference 1) can be easily ignored except by the most exacting requirements. The second-order interaction in Run 20 for a vector angle of 11.5° at the nominal axial load of 200 pounds was .00024 radian which agreed closely with the value of .00021 radian predicted for the basic design on Page 56 of Reference 1.

6.2 PRECISION OF THRUST MAGNITUDE

The precision of the strain gaged force links was adequate for the primary purpose of this experiment, which was to evaluate the structural geometry of the basic design. As shown in Table II, the 2σ precision of the resultant thrust for all combinations of axial and side loads was 0.14 percent The semiconductor strain gages evidenced a slight amount of creep under load (.03 percent for the first minute of loading for the axial force links). For this reason and because of the limited time available for the completion of the required number of tests, data was taken between one and two minutes after application of load, which did not always allow sufficient time for the weight pans to stop swinging. Generally, a calibration of this nature takes about two weeks including set-up time and re-runs, and undoubtedly the precision of the data shown in Table II, which was taken in the final two days of a five-day period, could have been improved had more time been available to improve calibration technique.

Under stress, creep of the epoxy bond between the strain gage and the substrate is always a potential problem in the manufacture of strain gage transducers. Metal foil strain gages are less subject to this effect than semiconductor gages because of the relative thickness of the constantan foil (.0001 inch compared to the silicon sliver, .0005 inch). However, semiconductor load cells are sufficiently free from creep if long gages are used and if proper attention is paid to the stress distribution along the strain gage. Given proper attention to these details, creep from semiconductor strain gages would be about .05 percent in five minutes[3]. Creep from constantan foil strain gages would be typically about .01 percent in the same period of time.

The strain gages used on the axial force links were somewhat non-linear as evidenced by the second-degree constants in the matrix in Table I (C_{11}, C_{22}, and C_{33}). This presented no problem since the method of data reduction provided for a second degree nonlinearity. The semiconductor gages used on the side force link were more linear as shown by the relative size of C_{44} to B_{44}. The nonlinearity may be calculated by 1/2 (EC/B) which is 0.11 percent of full scale for the side force link.

The first-order interaction of the side force link on axial force was reasonably small. This interaction is primarily caused by misalignment of the side force link as explained in Section 7.2.2., Ref. 1. This interaction is equal to $M_{14} + M_{24} + M_{34}$ (Table I) and is also equal to .0028 Fx/Fz. The maximum value of this would be 0.056 percent at a 11.5° vector angle. Again, this interaction was readily extracted from the data.

[3] Conversation by the author with John Pugnaire, Bytrex Division of Tyco Corp., Waltham, Mass.

6.3 PRECISION OF VECTOR LOCATION

Since the forces resolved by the three axial force links determine the location of the thrust vector in the xy plane of the balance, force link precision directly affects the precision of the measured vector location (see Section 7.1, Ref. 1). Consequently, the comments in the preceding paragraphs regarding precision also apply here. The precision obtained for the location of the thrust vector given in terms of the measured bias, and the 2σ variation of the vector location data in the last column of Table II was -.0024 inch $\pm$ .0003 inch.

Certain adjustments were made in the presentation of this data. After Run 18 it was noticed that the flexure connecting the axial force rod to the balance was bent. At this point a new flexure was installed and as a consequence the location bias was reduced by .008 inch. The second column for location error in Runs 12, 17, and 18, Table II, show this correction. After this adjustment the average of all runs (excluding 25 and 26) was -.0024 inch which can be partially attributed to errors in the measurement of the location of the three load stations (x_1, x_2 and x_3) for the axial calibrations. The last column in Table II shows the location errors corrected for this bias.

The location precision obtained was sufficient for the purposes of this experiment, which was primarily to evaluate the balance structural geometry. As with the precision of the thrust resultant, a five-to-one improvement in this location precision would be readily achieved by reduction of strain gage creep and by the improvement in calibration technique that would normally result from more experience with the calibration of this type of balance.

SECTION VII
CONCLUSIONS

An instrument designed in an orthogonal tripod geometry with short, rigid force-measuring links in a compact structure, can be used satisfactorily to measure the thrust vector (magnitude, direction, and location) produced by a rocket engine.

This type of vector thrust cell can also be conveniently calibrated with known axial and lateral loads in order to qualify the data obtained.

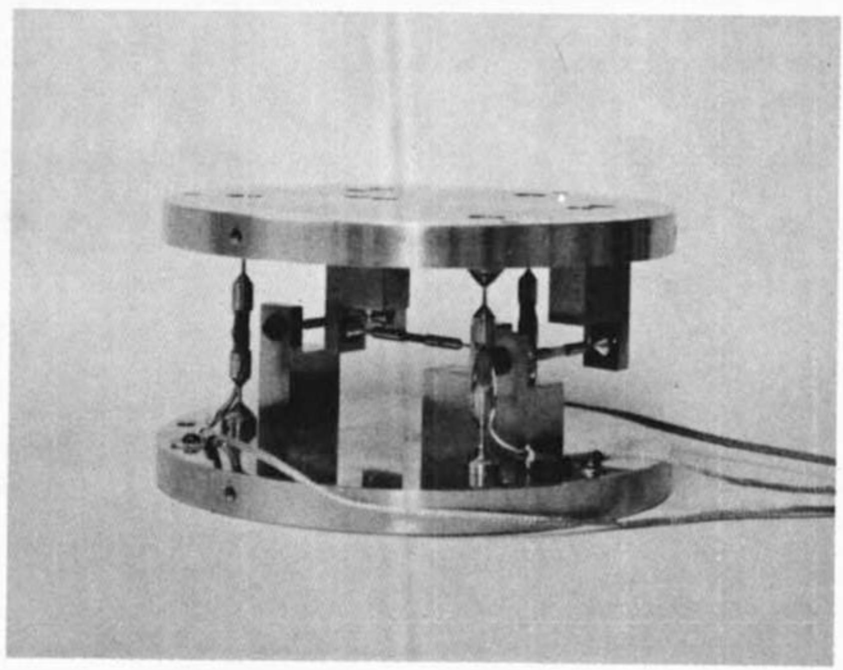

Figure 1. Scale Model Vector Thrust Load Cell

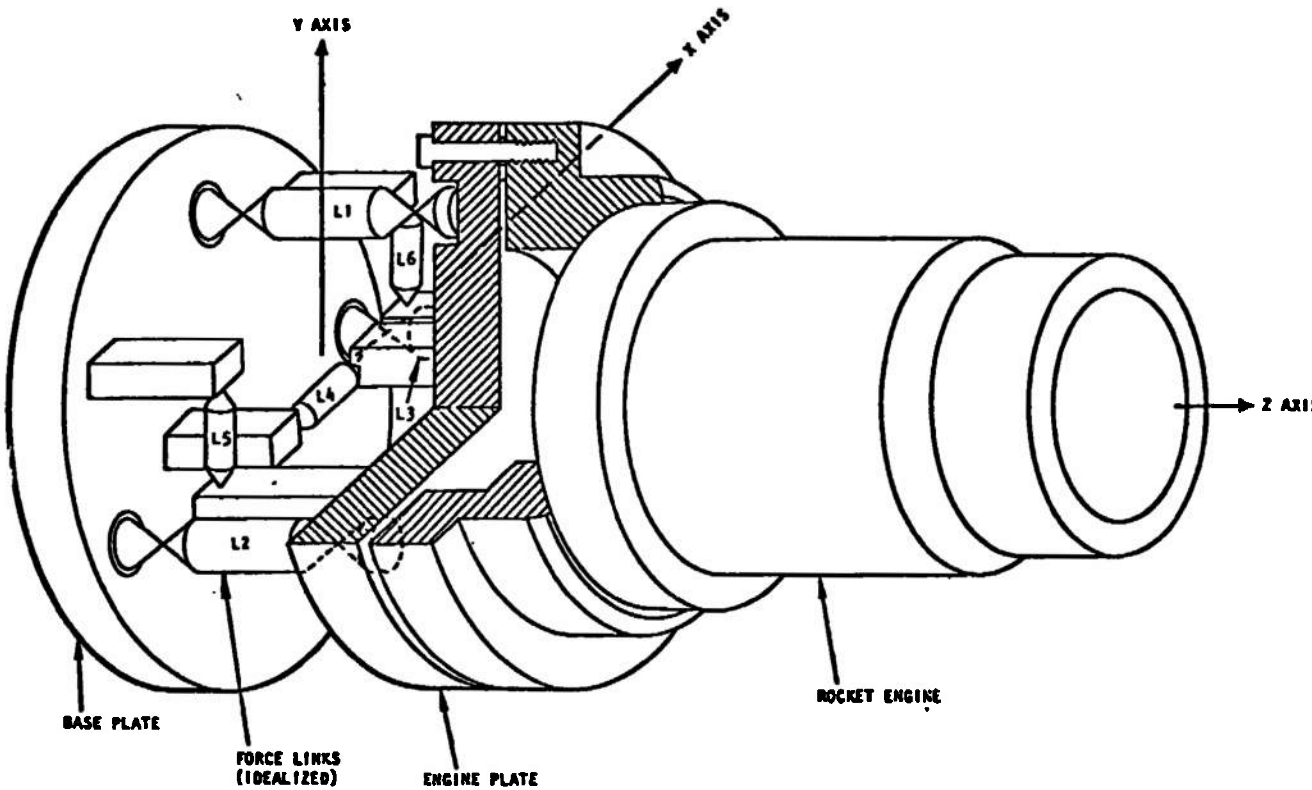

FIGURE 2. Force Link Arrangement of Model Cell

Axial Load (F_z)
Calibration Rod
and Flexure

Side Load (F_x)
Weight Pan

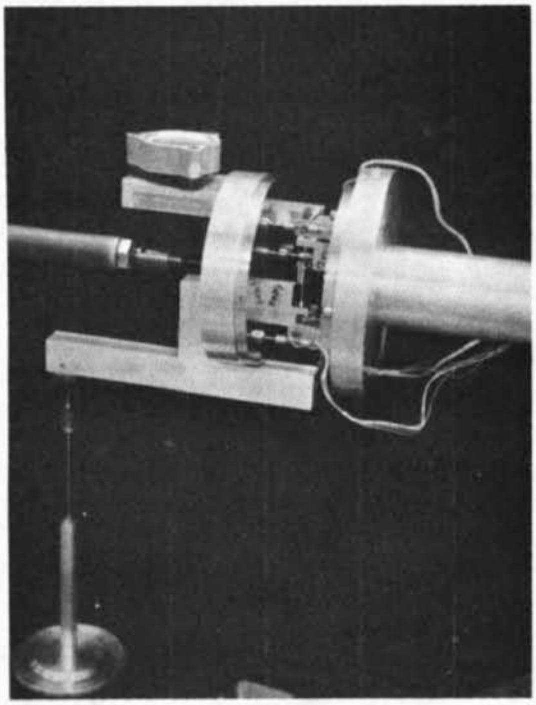

Movable Sting

Figure 3. Installation on Calibration Rig

UNCLASSIFIED
Security Classification

DOCUMENT CONTROL DATA - R & D

(Security classification of title, body of abstract and indexing annotation must be entered when the overall report is classified)

1. ORIGINATING ACTIVITY (Corporate author) North American Rockwell Corporation Rocketdyne Division, 6633 Canoga Avenue Canoga Park, California 91304	2a. REPORT SECURITY CLASSIFICATION UNCLASSIFIED 2b. GROUP N/A

3. REPORT TITLE
EXPERIMENTAL EVALUATION OF A THRUST VECTOR LOAD CELL

4. DESCRIPTIVE NOTES (Type of report and inclusive dates)
Final Report - November 1969 to February 1970

5. AUTHOR(S) (First name, middle initial, last name)
R. W. Postma, Rocketdyne

6. REPORT DATE	7a. TOTAL NO. OF PAGES	7b. NO. OF REFS
November 1970	25	None

8a. CONTRACT OR GRANT NO. F40600-70-C-0007 b. PROJECT NO. 4344 c. Program Element 65701F d. Task Nos. 37 and 08	9a. ORIGINATOR'S REPORT NUMBER(S) AEDC-TR-70-246 9b. OTHER REPORT NO(S) (Any other numbers that may be assigned this report) R-8254

10. DISTRIBUTION STATEMENT
This document has been approved for public release and sale; its distribution is unlimited.

11. SUPPLEMENTARY NOTES	12. SPONSORING MILITARY ACTIVITY
Available in DDC	Arnold Engineering Development Center, Air Force Systems Command, Arnold Air Force Station, Tenn.37389

13. ABSTRACT

This report describes the results of an experimental evaluation of a half-scale (physical size) model of a previously analyzed six-component force balance for testing rocket engines. The force range of the model was scaled down from 5000 lb_f to 200 lb_f, and structural parameters were scaled to represent those of the full-scale version which was analyzed under Contract F40600-68-C-0004. The evaluation includes the determination of (1) first- and second-order interactions of single and combination loads and (2) the effect of combination loads at expected gimbal points for typical rocket engines. The data which are presented in tabulated form, validate the prior analysis, and demonstrate that short force measuring links, assembled into a compact integral structure, do not result in excessive interactions.

DD FORM 1 NOV 65 1473

UNCLASSIFIED
Security Classification

14. KEY WORDS	LINK A		LINK B		LINK C	
	ROLE	WT	ROLE	WT	ROLE	WT
Model						
weight indicator						
load cells						
rocket engines						
gimbal						
force						

AFSC
Arnold AFS Tenn